A PARAMETRIC INVESTIGATION OF THE RESPONSE OF DIRECTLY LAMINATED COMPOSITE-TO-METAL SINGLE LAP JOINTS

V.A. Karatzas[1], Y. Zhang[2], N.G. Tsouvalis[1,*], M.K. Chryssanthopoulos[2]

[1] *National Technical University of Athens, School of Naval Architecture and Marine Engineering, Shipbuilding Technology Laboratory, Heroon Polytechniou 9, GR-15773 Zografos, Athens, Greece*
[2] *University of Surrey, Faculty of Engineering and Physical Sciences, Civil Engineering (C5), Guildford, Surrey, GU2 7XH, UK*
[*] *tsouv@mail.ntua.gr*

Keywords: Co-cured Joints, Single-lap, Hybrid, Adhesive Joints.

Abstract
Adhesive bonding is a rapidly growing technique that offers considerable potential to the repairing and joining of structural members. This work has been performed within the context of FP7 Co-Patch research program and presents a parametric experimental study of adhesively bonded single lap joint geometries between dissimilar materials, namely typical marine steel and carbon fiber reinforced polymers, using the co-curing technique i.e. by directly laminating the composite on the steel. Four different geometry cases with varying overlap and substrate lengths and five different composite material systems were considered and experimentally tested. It may be concluded that the failure load of the joints increased with the increase of the overlap length. The magnitude of this increase is strongly dependant on the quality of bonding over the overlap length, which in turn is associated with the fabrication method, rather than the mechanical properties of the composite material system..

1 Introduction
Composite material systems have been used in a plethora of advanced engineering structures as they are versatile, lightweight and exhibit remarkable mechanical properties. Advances in engineering and composite materials science rendered feasible the replacement of metal components in structures by composite materials. Therefore composite joint design has become a very important research area, as these joints are generally the weakest part of composite and hybrid structures. The most common types of joining methods in composite structures are mechanical joining and bonding. Mechanical fastening rely on mechanical means such as rivets or bolts, which in most cases require drilling holes. Although this method makes the disassembly and the inspection easier, it also leads to undesirable stress concentrations, increase of weight of the structure and non-uniform load transfer through the joint. On the contrary, adhesive joints provide a more uniform load transfer and do not add to the weight of the structure, while rivets or bolts, where stress concentrations appear, are not required. Moreover, it is an ideal method for joining different materials, especially composite materials to metallic ones. For these reasons, adhesively bonded joints are increasingly being utilized substituting traditional methods of bonding such as welding, fastening and bolting. On the other hand, adhesive bonding presents several disadvantages as it is sensitive to

environmental conditions, both during manufacturing and in service and the appropriate surface treatment, which depends on the type of the adherents, is crucial for the good performance of the joint. Furthermore, the manufacturing procedure is more complicated compared to fastened joints. One type of adhesive bonding is the co-cured joining method. Co-cured joints use the excess resin of the composite system during the curing process as the adhesive. This method presents several advantages compared to adhesively bonded joints where a different adhesive is used, as the design, analysis and manufacturing of these kind of joints is simpler compared to adhesive joints, it requires no surface preparation of the composite adherent and it is considerably faster, as the bonding process is performed simultaneously to the curing process of the composite system.

Despite the aforementioned advantages, only a few studies on co-cured joints are available. Shin et al [1] fabricated and tested in tension co-cured single-lap and double-lap joints between composite pre-preg and steel and investigated the failure mechanisms with the use of finite element models and failure criteria. The same author investigated the effect of thermal residual stresses on failure of co-cured lap joints under static and fatigue tensile loads [2]. Park et al [3] investigated both experimentally and analytically a series of design parameters with respect to the stacking sequence and the thickness ratio of the adherents for co-cured aluminum to carbon epoxy composite double lap joints in tension and fatigue. Russo and Zuccarello [4] studied the influence of the resin layer at the interface of hybrid metal to composite co-cured joints and showed that in general the effect of the resin thickness is negligible when it is not greater than 0.1 mm. Kweon et al [5] performed a large series of experiments investigating different parameters such as the overlap length, the stacking sequence and the adherent thickness for four different manufacturing methods and their effect on the shear strength of composite single lap bonded joints. The results showed that co-cured joints showed higher strength than the other manufacturing methods. In a subsequent work, the same author [6] studied the effect of various environmental conditions on the strength of carbon epoxy composite single lap joints that were manufactured using four different manufacturing methods. An area where the co-cured joining method presents significant interest due to its advantages is composite patch repairing of defected metallic structures. Unfortunately, only a few studies can be found in the literature addressing this issue. Typical examples are the works of Grabovac [7-8], where a ship superstructure that was prone to fatigue-induced cracking has been reinforced with a composite reinforcement whose adhesive and matrix systems are the same. No further cracking has occurred in the rehabilitated structure over a 7-year period that the ship was in service and the repair remained in good condition despite exposure to a severe marine environment.

The work presented in this article has been performed within the context of FP7 Co-Patch research program (Composite Patch Repair for Marine and Civil Engineering Infrastructure Applications, www.co-patch.com) and presents a parametric experimental study of adhesively bonded single lap joint geometries between dissimilar materials, namely typical marine steel and carbon fiber reinforced polymers, where the composite is directly laminated on the steel. The purpose of this study is to extract valuable knowledge for this specific type of adhesive bonds that will be used in the design and application criteria of composite patches for the rehabilitation of defected steel structures in future tests. Four geometry cases with varying overlap and substrate lengths for three different composite materials and three different fabrication methods were considered and experimentally tested.

2 Specimen geometry

In order to investigate the effect of the overlap length on the strength of the joint, four different geometry cases have been tested in tension. The overlap length varied from short with a 12.5 mm length (case A), increasing to intermediate (100 mm overlap for case B) and finally long overlaps (200 mm for case C and 300 mm for case D). It was decided that the ratio of the overlap length to the free adherent length between the tabs and the overlap equals 2 for cases B, C and D, based on the corresponding relation defined in ASTM D 5868 [9] for metal to composite single lap shear joints testing. However, for case A, due to the short overlap, the aforementioned ratio would lead into unrealistic dimensions and therefore a different value was selected. The width of the specimens was equal to 25 mm for all cases and the dimensions of each geometry case are shown in Figure 1 and listed in Table 1. Strain gages have been used in appropriate positions so as to provide insight on the crack initiation and propagation in the overlap area and for the validation of the experiments with finite element models in future studies. The strain gages positions are depicted in Figure 1.

	Geometry Case			
	A	**B**	**C**	**D**
L_{OV} [mm]	12.5	100.0	200.0	300.0
L_C [mm]	50.0	50.0	100.0	150.0
L_{St} [mm]	50.0	50.0	100.0	150.0
L_{TSt} [mm]	50.0	50.0	50.0	50.0
L_{TC} [mm]	50.0	50.0	50.0	50.0
t_C [mm]	5.0	5.0	5.0	5.0
t_{St} [mm]	7.5	7.5	7.5	7.5

Table 1. Dimensions of specimens.

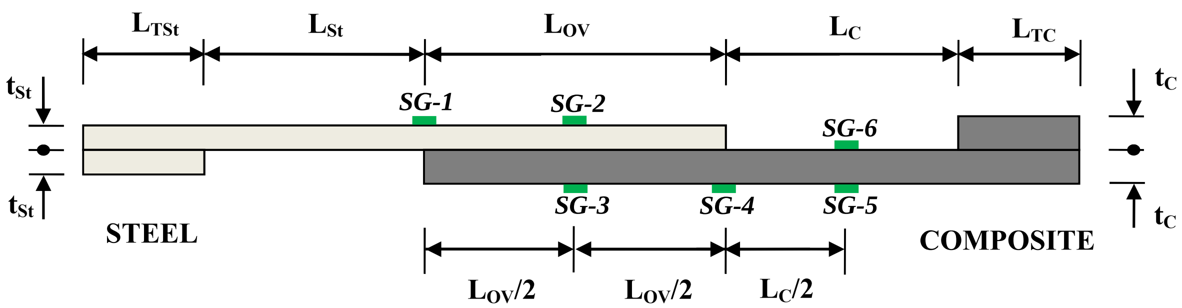

Figure 1. Principal dimensions of specimens and positions of strain gages.

3 Materials

In total, five distinct composite material systems were examined, considering the variations in both the material selection and the fabrication method. In particular, the composite systems tested were: carbon/epoxy using the hand-lay-up method (HLU-C/E), carbon/vinylester using the hand-lay-up method (HLU-C/V), carbon/epoxy using the vacuum infusion method (VI-C/E), carbon/vinylester using the vacuum infusion method (VI-C/V), and carbon/epoxy pre-preg (PP-C/E). The composite substrate was in all cases comprised of unidirectional plies that had the fiber direction parallel to the length of the specimens. In each case the appropriate number of plies was used so as to reach the desired laminate thickness of 7.5 mm. Details about the types of fibers and the resins used are concentrated in Table 2. The steel used was typical marine steel. The mechanical properties of the materials have been measured from a preceding series of characterization tests and are listed in Table.

MATERIALS								
Method	Composite System	Carbon Fibers		Resin		Glass Fibers insulating layer		
		Type	*Supplier*	*Type*	*Supplier*	*Type*	*Supplier*
Hand Lay-Up	Carbon/Epoxy **HLU-C/E**	CST 200 one layer 200 g/m^2	SGL	LH 160 133-138 Hardener	HAVEL + HEXION	Twill fabric 280g/m^2	AEROGLASS
	Carbon/Vinylester **HLU-C/V**	L(X) 440-C10 $[0]_2$, 208 g/m^2 each	AMT DEVOLD	DION 9500-M800	REICHHOLD	Chopped Strand Mat 300 g/m^2	SG VETROTEX
Vacuum Infusion	Carbon/Epoxy **VI-C/E**	CST 200 one layer 200 g/m^2	SGL	LH 288 H 281-283 Hardener	HAVEL + HEXION	Twill fabric 280g/m^2	AEROGLASS
	Carbon/Vinylester **VI-C/V**	L(X) 440-C10 $[0]_2$, 208 g/m^2 each	AMT DEVOLD	DION 9500-501	REICHHOLD	Chopped Strand Mat 300 g/m^2	SG VETROTEX
Pre-preg	Carbon/Epoxy **PP-C/E**	HS 40, 300 g/m^2	Grafil Inc.	SE84LV	SP Gurit	DB 810-E05 HD 45/0/-45, 809 g/m^2	AMT DEVOLD

Table 2. Details of the materials used for the composite adherent.

Properties	HLU-C/E	HLU-C/V	VI-C/E	VI-C/V	PP-C/E
E_{1T} [GPa]	38.7±1.8	74.0±3.2	112.3±11.93	102.6±8.7	228.4±6.4
E_{2T} [GPa]	6.5±0.5	5.1±0.2	5.5±0.4	7.6±0.8	6.5±0.4
ν_{12}	0.36	0.39	0.38	0.49	0.25
G_{12} [GPa]	1.7±0.1	2.5±0.1	2.0±0.2	4.5±0.1	4.5±0.1

Table 3. Mechanical properties of the composite materials.

4 Fabrication procedure

For the fabrication of the specimens for each material configuration and geometry case, larger panels were made from which the specimens were cut in the required dimensions using water jet cutting. The general procedure for the fabrication of these plates consists of the following steps (Figure 2). The overlap area of the steel plate was grit blasted to SA2½ surface roughness and the plate was positioned on the workbench. A release agent was applied on the steel plate after protecting the overlap area with a vinyl tape. The vinyl tape guaranteed that there will be no release agent in the overlap area that would jeopardize the integrity of the bond and also created a sharp edge towards the overlap area once it was removed. An auxiliary plate was positioned exactly next to the steel, thus providing the support to the composite system during its lamination and curing; therefore particular attention was given so that the auxiliary plate has the same thickness with the steel plate and larger dimensions than the overall length of the composite substrate. On top of the auxiliary plate, a release agent was applied to facilitate its removal after the procedure and the composite layers were laminated directly on the steel surface and the auxiliary plate's surface. A first resin rich layer was applied in all cases to ensure that there would be no dry spots/unbounded area in the overlap. The single glass fiber layer was in all cases laminated using the hand-lay-up technique regardless of the fabrication technique of the composite adherent. Subsequently the carbon layers were laminated. The laminates were left to cure in room conditions for 24 hours, the temperature varying between 15 – 25^{o}C and the relative humidity 45-75%; the pre-preg specimens were cured under a constant vacuum pressure of -0.95 bar with a mean curing temperature of 86.4^{o}C for 10 hours. After curing, the edges of the composite adherent were trimmed in both ends in order to have a sharp profile and have constant thickness throughout the composite material. The edge of the composite that was at the end of the overlap was trimmed with caution avoiding damaging the bond or the metal surface. The steel and composite tabs were bonded in their right location by using an adhesive. Some typical parent panels are shown in Figure 3. After the curing of the adhesive in the tab areas, the specimens were cut from the parent plates in the required dimensions using water jet cutting. Four specimens were fabricated for each geometry-material configuration resulting in totally eighty specimens. The overall quality of the specimens ranged from mediocre to satisfactory. The project partners responsible for the fabrication were AS2CON, ENP, NTNU and UM (refer to www.co-patch.com for the partners' details).

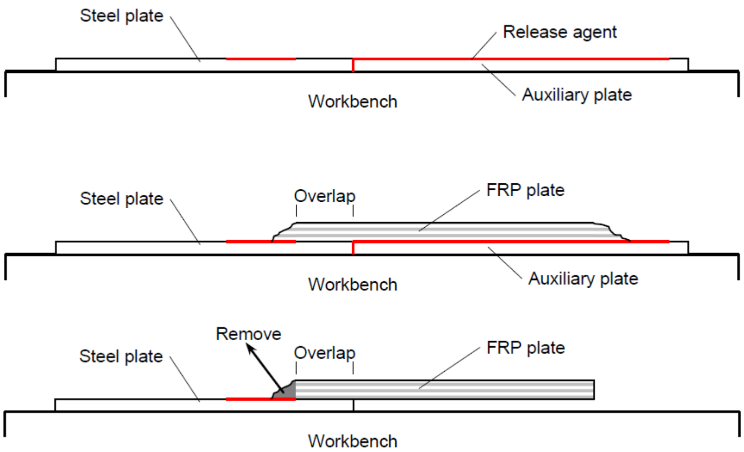

Figure 2. Fabrication stages of the parent panels.

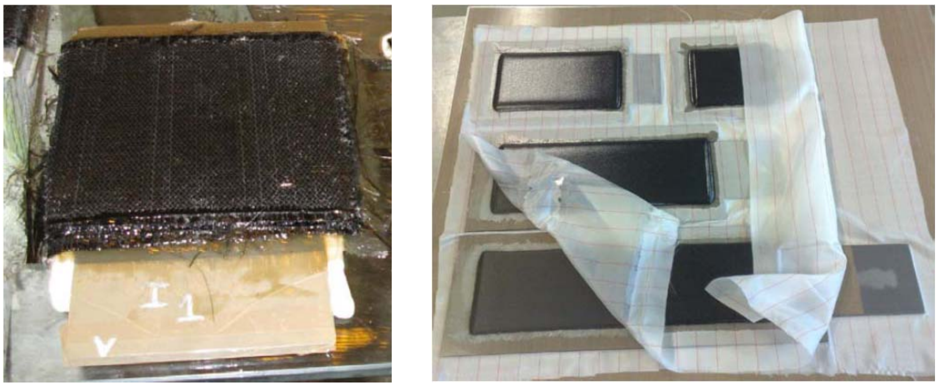

Figure 3. HLU-C/V-A case parent panel lamination and PP-C/E panels after curing.

5 Test parameters and results

Three out of the four specimens produced for each case were tested. The tensile tests were performed using displacement control, the rate varying depending on the time needed for the failure of each type of specimen. In the majority of the cases the testing rate was either 0.5 mm/min or 1 mm/min. During testing, the force, crosshead displacement and the measurements from the strain gages were recorded.

In every case failure started from the edge of the overlap area and, for the small overlap lengths (cases A and B), was instantaneous. In geometry cases C and D debonding propagated along the bondline until the ultimate failure of the bond. In general two dominant modes of failure were observed. The first one was fiber-tear failure in which the delamination occurred between the insulation glass fiber layer and the carbon fiber laminate. Some glass fibres, or even most of the glass fiber layer (see Figure 4(up)), had been peeled off and were stuck on the surface of the steel substrate. The second mode was interfacial failure between the glass fiber layer and the steel surface (Figure 4(down)). Here, after the separation of specimen parts, there was almost no or just a very small amount of fibre and/or resin left on the grit blasted surface of the steel substrate.

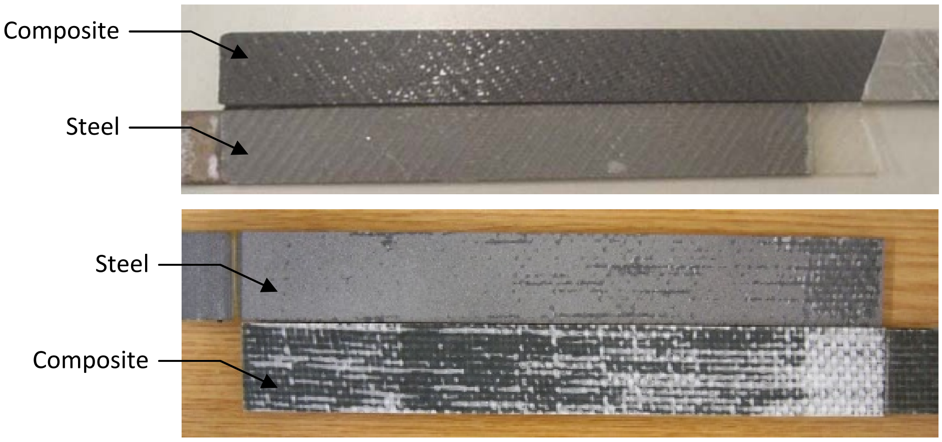

Figure 4. Typical failure modes: fiber-tear failure (up) and interfacial failure (down).

The force-crosshead displacement curves for two selected material cases (HLU-C/V and VI-C/V) are presented in Figures 5(a) and (b). The slope of the initial linear part of the load-displacement curves can be considered as the stiffness of the joints prior to crack initiation. As indicated by Figure 5(b), the joint stiffness exhibited an increasing trend as we move to shorter overlap length, from case D to case B. By contrast, for case A with the shortest overlap, the joint stiffness remained similar to case B. This observation agreed well with the finite element modeling which is not included in this paper. The aforementioned trend, however, was not observed for the HLU-C/V series of tests (see Figure 5(a)). Here, the joint stiffness does not appear to increase by decreasing the overlap length, which is believed to result from the variability in the fabrication quality of the hand lay-up method, particularly when the overlap is short.

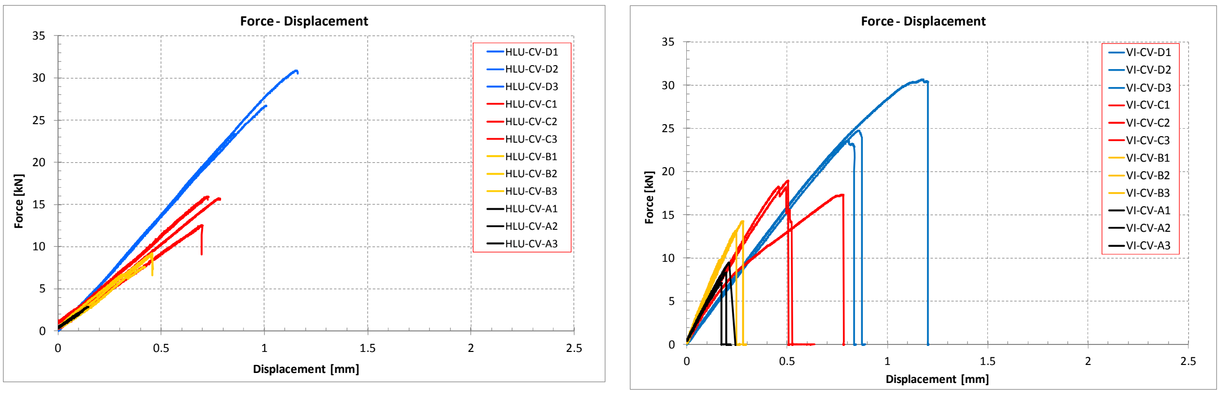

(a) (b)

Figure 5. Force – Crosshead Displacement graphs for selected material cases: (a) HLU-C/V and (b) VI-C/V.

The average failure loads of all specimens are listed in Table 4. Interestingly the HLU-C/E specimens exhibited a higher failure load than the HLU-C/V, VI-C/E and VI-C/V specimens in almost all geometry cases. Overall, the carbon/epoxy composite system yielded higher failure loads than the carbon/vinylester for specimens with longer overlap length where the influence of the fabrication variability was fairly little. By assigning the overlap length and failure loads of Case A as a benchmark, the corresponding failure load ratios of the other three cases are plotted in Figure 6. Overall, the failure load of the joints reveals an increase with the increase of the overlap length for all test series with the exception of PP-C/E. As revealed from the inspection of the overlap area of these specific specimens after testing, this was caused by the poor bonding of the composite substrate to the steel which allowed the ingress of water during water jet cutting. It is also noticed in Figure 6 that the enhancement of failure loads due to the increasing overlap length was more significant for the hand lay-up specimens compared to those made through vacuum infusion. Most remarkably, for the HLU-C/V series, the failure load was increased by more than tenfold between geometry case A and case D. This may be seen as further evidence of the highly variable fabrication quality of the hand lay-up method for joints with very short overlap, i.e. case A, which had also been revealed by the observations made with respect to the load-displacement plots of the HLU-C/V material case (see Figure 5(a)).

Failure Loads [kN]				
Material	**Geometry Case**			
	A	**B**	**C**	**D**
HLU - C/E	6.00±0.58	17.77±0.95	25.10±2.52	43.40±1.39
HLU - C/V	2.42±0.36	7.52±1.41	15.14±2.11	26.66±3.55
VI - C/E	7.22±1.28	14.39±1.00	18.15±0.30	38.46±1.71
VI - C/V	8.32±1.18	14.02±0.78	18.15±0.79	26.32±3.83
PP - C/E	7.89±1.15	23.42±1.43	11.78±1.60	16.89±2.81

Table 4. Average failure loads of the tested specimens.

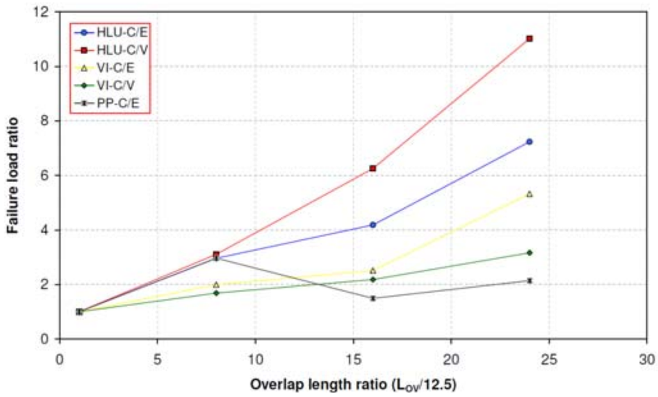

Figure 6. Ratio of failure loads VS. ratio of overlap length of the tested specimens.

Typical strain measurements are plotted versus the applied force in Figure 7. The strain gages in positions SG1 and SG4, so-called back-face strain gages, exhibited a sudden change of the strain following from the initial linear pattern. This can be considered as an indication of the onset of damage when debonding started due to the fact that the load is no longer transferred as effectively through the bond to both substrates. On the other hand, for the strain gages in position SG5 an almost linear behavior was observed through the entire load application procedure, see Figure 7.

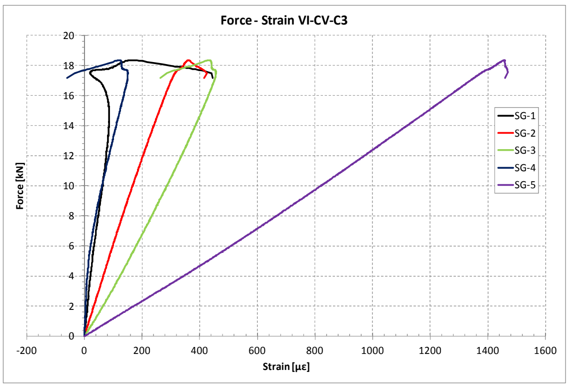

Figure 7. Typical force – strain graphs.

6 Conclusions

The effects of overlap length on the stiffness and failure loads were experimentally investigated for a range of co-cured adhesively bonded single lap joints, which were classified into five distinct composite material systems, considering both material properties and fabrication method. Fiber-tear failure and interfacial debonding were the two major failure modes observed in these tests. From the evaluation of the results, it is evident that the failure load increases as the overlap length increases, provided the quality of the fabrication method can be assured throughout the overlap range; however, this increase in the load bearing capacity of the bonded joint is not directly proportional to the increase in the overlap length. Concerning the method used for the fabrication of the specimens, observations on both joint stiffnesses and failure loads suggest that there is higher variability in the fabrication quality of the hand lay-up method for joints with very short overlap. Finally, concerning the appropriateness of strain measurements in lap joint behavior, it was demonstrated that the back-face strain gages exhibit a sudden change of strain which can be used to detect the initiation of damage, and therefore, whether the failure of the joint occurs suddenly or through a process of debonding propagation.

Acknowledgments

The research leading to these results has received funding from the European Community's Seventh Framework Programme (FP7/2007-2013) under grant agreement n° 233969 (www.co-patch.com). The authors gratefully acknowledge the contribution of project partners AS2CON (A. Klanac and D. Bolf), ENP (G.P. Cabral), ISQ (G.F. Pimenta), NTNU (A. Echtermeyer and J.H.L. Grave) and UM (T. Helland).

References

[1] Shin K.C., Lim J., Lee J. The manufacturing process of co-cured single and double lap joints and evaluation of the load-bearing capacities of co-cured joints. *Journal of Materials Processing Technology*, **138**, pp. 89-96 (2003).

[2] Shin K.C., Lee J.J. Effects of thermal residual stresses on failure of co-cured lap joints with steel and carbon fiber–epoxy composite adherends under static and fatigue tensile loads. *Composites: Part A: Applied Science and Manufacturing*, **37**, pp. 476–487 (2006).

[3] Park S.W., Kim H.S., Lee D.G. Optimum design of the co-cured double lap joint composed of aluminum and carbon epoxy composite. *Composite Structures*, **75**, pp. 289-297 (2006).

[4] Russo A., Bernardo Zuccarello B. Influence of the Resin Layer Thickness at the Interface of Hybrid Metal-composite Co-cured Joints. *Procedia Engineering*, **10**, pp. 3775–3786 (2011).

[5] Song M.G., Kweon J.H., Choi J.H., Byun J.H., Song M.H., Shin S.J., Lee T.J. Effect of manufacturing methods on the shear strength of composite single-lap bonded joints. *Composite Structures*, **92**, pp. 2194–2202 (2010).

[6] Park Y.B., Song M.G., Kim J.J., Kweon J.H., Choi, J.H. Strength of carbon/epoxy composite single-lap bonded joints in various environmental conditions. *Composite Structures*, **92**, pp. 2173-2180 (2010).

[7] Grabovac I. Bonded composite solution to ship reinforcement. *Composites: Part A: Applied Science and Manufacturing*, **34**, pp. 847-854 (2003).

[8] Grabovac I., Whittaker D. Application of bonded composites in the repair of the ships structures – A 15-year service experience. *Composites: Part A: Applied Science and Manufacturing*, **40**, pp. 1381-1398 (2009).

[9] ASTM D 5868 – 01. *Standard Test Method for Lap Shear Adhesion for Fiber Reinforced Plastic (FRP) Bonding* (2008).